# Altered dynamics of neurovascular coupling in CADASIL

Clément Huneau, Marion Houot, Anne Joutel, Benoit Béranger, Christian Giroux, Habib Benali, Hugues Chabriat

ANNALS of Clinical and Translational Neurology
Open Access
ANA American Neurological Association since 1875

RESEARCH ARTICLE

# Altered dynamics of neurovascular coupling in CADASIL

Clément Huneau[1,2], Marion Houot[3], Anne Joutel[4], Benoit Béranger[5], Christian Giroux[6], Habib Benali[2,7] & Hugues Chabriat[4,6]

[1] Laboratoire des Sciences du Numérique de Nantes - LS2N, Centre National de la Recherche Scientifique UMR6004, Université de Nantes, Nantes, France
[2]Laboratoire d'Imagerie Biomédicale, Centre de la Recherche Scientifique UMR7371, Inserm UMR1146, Université Pierre et Marie Curie Paris VI, Paris, France
[3]Centre of Excellence of Neurodegenerative Disease - CoEN, ICM, APHP Department of Neurology, Hôpital Pitié-Salpêtrière, Institute of Memory and Alzheimer's Disease - IM2A, University Paris 6, Paris, France
[4]Sorbonne Paris Cité, Inserm UMR1161, Université Denis Diderot Paris VII, Paris, France
[5]Centre de Neuro-Imagerie de Recherche - CENIR, Institut du Cerveau et de la Moelle épinière - ICM, Paris, France
[6] Département de Neurologie and DHU NeuroVasc, AP-HP, Hôpital Lariboisière, Paris, France
[7]Faculty of Engineering and Computer Science, University Concordia, Quebec, Canada

**Correspondence**
Hugues Chabriat, Dept Neurology, Hopital Lariboisiére (Université Denis Diderot Paris 7), 2 rue A Paré, 75010 Paris, France. Tel: 33 1 49952593; Fax: 33 1 49952596; E-mail: hugues.chabriat@aphp.fr

**Funding Information**
This study was supported by grants from the Fondation Leducq (Transatlantic Network of Excellence on the Pathogenesis of Small Vessel Disease of the Brain; http://www.fondationleducq.org), ANR (Ministry of Health and Research, (Commissariat General à l'Investissement) RHU TRT_cSVD). Clement Huneau was funded successively by Fondation de l'Avenir and by the Leducq Foundation.

Received: 10 April 2018; Accepted: 13 April 2018

***Annals of Clinical and Translational Neurology*** **2018; 5(7): 788–802**

doi: 10.1002/acn3.574

## Abstract

**Background and Objective**: Neurovascular coupling is the complex biological process that underlies use-dependent increases in blood flow in response to neural activation. Neurovascular coupling was investigated at the early stage of CADASIL, a genetic paradigm of ischemic small vessel disease. **Methods**: Functional hyperemia and evoked potentials during 20- and 40-sec visual and motor stimulations were monitored simultaneously using arterial spin labeling-functional magnetic resonance imaging (ASL-fMRI) and electroencephalography. **Results**: Cortical functional hyperemia differed significantly between 19 patients and 19 healthy individuals, whereas evoked potentials were unaltered. Functional hyperemia dynamics, assessed using the difference in the slope of the response curve between 15 and 30 sec, showed a time-shifted decrease in the response to 40-sec neural stimulations in CADASIL patients. These results were replicated in a second cohort of 10 patients and 10 controls and confirmed in the whole population. **Interpretation**: Alterations of neurovascular coupling occur early in CADASIL and can be assessed by ASL-fMRI using a simple marker of vascular dysfunction.

## Introduction

The cerebral microvasculature is responsible for delivering a continuous supply of energy to brain cells through two major, intricately regulated mechanisms: cerebral autoregulation and functional hyperemia.[1] These mechanisms are engaged in response to complex signaling pathways elicited at the level of the neurovascular unit, comprising neuron terminals and astrocytes, as well as endothelial cells, smooth muscle cells and pericytes within the wall of microvessels.[2] The biological processes underlying the changes in vascular diameter and resulting hyperemia during neural activation are referred to as neurovascular coupling (NVC).[1]

CADASIL (Cerebral Autosomal Dominant Arteriopathy with Subcortical Infarcts and Leukoencephalopathy) is the most frequent mendelian type of cerebral small vessel disease (SVD) and represents a unique model for studying NVC in ischemic SVDs.[3,4] Preclinical studies recently showed that all mutations in CADASIL lead to aggregation of NOTCH3 extracellular domains (ECD) into multimeric species that form complexes with different binding partners

in the wall of microvessels.[5] An early reduction in functional hyperemia in response to whisker stimulation has consistently been observed in CADASIL mice prior to overt smooth muscle cell loss.[6,7] Importantly, recent studies have shown that these NVC alterations result from the disruption of signaling pathways secondary to NOTCH3-ECD accumulation.[6,8] Alterations in NVC may therefore represent one of the earliest physiological manifestations of the disease.

Changes in NVC in vivo can be probed using functional magnetic resonance imaging (fMRI) techniques.[9] A reduction in the blood oxygenation level-dependent response (BOLD) after various stimulations has been recently reported in patients with probable cerebral amyloid angiopathy (CAA)[10] and in few individuals with sporadic SVD.[11] However, there are many hurdles for interpreting these previous fMRI data. For example, the use of BOLD contrast precludes determination of whether the reduced response is attributable solely to local changes in blood flow or to altered oxygen use or exchange.[12] The BOLD response, which presumably originates from changes in blood volume in the venous compartment, also appears to be relatively insensitive to increases in capillary blood flow.[13,14] In addition, the possibility that a diminished neural response is the main driver of the reduced increase in flow observed in previous studies cannot be excluded in the absence of a separate, independent evaluation of neuronal activity.

Other fMRI methods allow the observation of purely hemodynamic changes at the cerebral level that are not sensitive to oxygenation level. Among them, arterial spin labeling (ASL) can be easily used to measure variations in cerebral blood flow (CBF), although at lower temporal resolution than is possible with BOLD fMRI.[15–17] Importantly, electroencephalography (EEG) can now be performed simultaneously with ASL-fMRI to provide an independent measure of neural activity at the cortical level in parallel with hemodynamic changes.[18]

In this study, we used ASL-fMRI combined with EEG to investigate NVC responses to two types of neural stimulations – visual and motor – obtained over short and long-time frames at an early stage of CADASIL.

## Materials and Methods

### Subjects

CADASIL patients were included in the study based on the following criteria: (1) age between 30 and 60 years, (2) no current cognitive or motor complaints, (3) no significant disability and a modified Rankin Scale (mRS) of 0 or 1, and (4) no focal neurological deficits at clinical examination. Age- and sex-matched healthy controls without any history of neurological disorder were recruited in parallel (see results paragraph). Neither patients nor controls had been treated with any antihypertensive agents or drugs with vasoactive properties (serotonin, dopamine, norepinephrine, phenylephrine or adrenaline) prior the MRI examination. The use of aspirin, clopidogrel, or antidepressant drug was tolerated. Current smokers could participate in the study, but only if they agreed to discontinue their tobacco use at least 1 day before the examination. Informed and written consent was obtained from all subjects. The study protocol was approved by an independent Medical Ethics Committee.

### Stimulation protocol

The functional MRI study was based on repeated visually cued motor tasks (Fig. 1A). The subject was asked to perform simple opening-closing hand movements during the period when a flickering (6 Hz) black/white (100% contrast) checkerboard was displayed on a screen and to stop these movements as soon as a white cross was displayed on the black background. The subject had to use his/her nondominant hand during all stimulation sequences and was trained for a few minutes to perform the hand movements at a stable frequency of 1 Hz prior to commencing acquisitions. A total of six, 5-min stimulation sequences were performed. Each sequence was composed of four activation periods lasting 20 sec ($n = 2$) or 40 sec ($n = 2$), randomly distributed and interleaved with four rest periods (Fig. 1B). The rest periods lasted 40 sec plus a random jitter varying from 0 to 2.76 sec.

### Electroencephalography

During ASL-fMRI experiments, electrical activity of the brain was recorded in all participants using electroencephalogram (EEG). Before the subject was placed inside the MRI scanner, they were equipped with an MRI-compatible, head-size–adjustable electrode cap (BrainCap-MR 64Ch-standard; EASYCAP Gmbh; Fig. 1C). This cap allowed recording of 63 EEG (10–20 system) channels and contained a reference and a ground electrode positioned over the fronto-central cortex. Impedance between electrodes and the reference was kept below 10 kΩ. Electrical signals were recorded at 5 kHz using two 32-channel amplifiers, with the battery placed close to the subject (BrainAmp MR plus; Brain Vision LLC) and linked to the BrainVision acquisition software. Electrophysiological recordings were performed during all fMRI sequences.

### MRI acquisition

Subjects were placed in a 3T MRI scanner (Magnetom Verio; Siemens Healthcare, Erlangen, Germany) and were

 

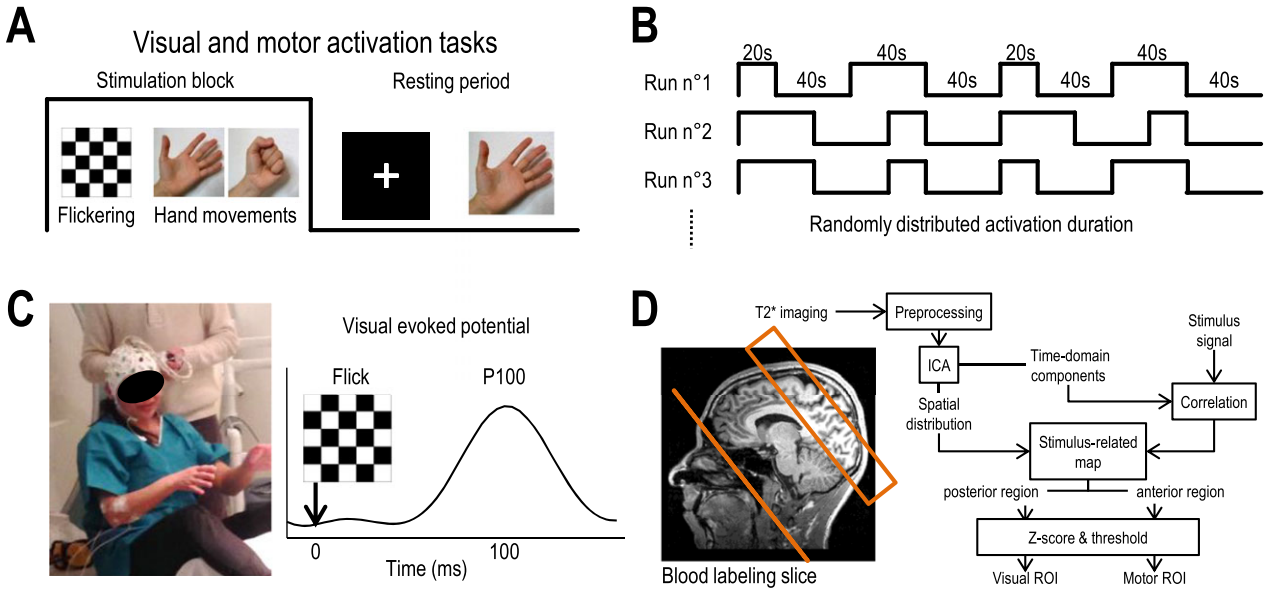


**Figure 1.** Neural stimulation procedures, acquisition protocol and selection of regions of interest. (A) Visual and motor cortex areas were simultaneously activated with a visually cued motor task. The visual stimulation used was a black and white checkerboard flickering at 6 Hz. The motor task was an open-close hand movement performed at 1 Hz. (B) 20- and 40-sec stimulation blocks were randomly distributed and interleaved with 40-sec rest periods. (C) EEG recording during the fMRI experiment allowed measurement of the P100 wave (at 100 msec) from visual evoked potentials during visual stimulations. (D) Schematic summary of the pseudo-continuous arterial spin labeling (pCASL) fMRI imaging protocol and processing procedure. Labeling slice and imaged field of view of the pCASL sequence are shown projected on a T1-weighted image from a control subject. ICA: independent component analysis.

first trained to perform hand movements while lying inside the MRI scanner. After subjects were positioned in the scanner, a full brain T1-weighted magnetization-prepared rapid gradient echo (MPRAGE) was acquired. CBF and BOLD signal variations were simultaneously monitored using pseudo-continuous ASL (pCASL) with T2*-weighted echo planar imaging (EPI) (1) using the following settings: label duration = 1500 msec; postlabeling delay = 900 msec; TR = 2760 msec; TE = 10 msec. For each subject, the field of view (FOV; 6 slices, thickness = 7 mm, gap = 0.35 mm; 4 mm² 64 × 64 matrix) was positioned using the T1 volume containing both the primary motor (M1) and visual (V1) areas (Fig. 1D, left). Blood flow measurements were calibrated on a voxel-by-voxel basis using proton-density images (EPI; TR = 10,000 msec; TE = 10 msec) obtained in the previous FOV T2*-weighted EPI images were obtained using the pCASL acquisition parameters (TR = 2760 msec; TE = 10 msec) over the entire brain (20 slices).

## MRI Data Analysis

### Preprocessing

MRI preprocessing was performed using MATLAB with the SPM12 toolbox. All fMRI data were first realigned to correct for head movements that occurred during the study. The corresponding images were registered to T1-weighted images (anatomy) using the full brain T2* sequence (see MRI acquisition, above). Calculation of blood flow signals was performed by subtracting the previous and subsequent tagged image from each control image, thereby preserving time sampling. CBF signals were then expressed as milliliters per gram per minute (mL/100 g/min), assuming a blood-brain partition of 0.9 mL/g, a blood T1 of 1650 msec, and a labeling efficiency of 0.68.[15]

### Regions of interest

An ROI was delineated in both V1 and M1 areas based on the detection of blood flow changes that correlated with the stimulation paradigm (Fig. 1D, right). This detection was automated and was obtained separately for each subject using a spatial independent component analysis. First, merged blood flow series were bandpass filtered (cutoff frequencies: [0.01; 0.1] Hz) to eliminate remaining motion noise and slow variations. Filtered signals were then decomposed into 40 independent time-domain components based on the Infomax algorithm.[19] The correlation of each component with the stimulation paradigm was then calculated. For the most-correlated components,

 

the map of their distribution at the voxel level was used to determine activated voxels. The center of the FOV on the anteroposterior axis was used to separate the anterior and posterior parts of the stimulus-related map. Each part was then normalized separately and used to build two z-score maps; this separation was performed based on the assumption that, with normalization, visual activation might alter the detection of motor activation, and vice versa. A Z-score threshold > 3 was chosen for delineating motor and visual ROIs in activated motor and visual areas in each subject. The detection of ROIs was performed using the MATLAB Software and the NEDICA toolbox.[20] The sizes of ROIs in patient and control populations were compared using a two-sided Student's *t*-test.

### Statistical analysis of baseline blood flow

Resting state CBF during fMRI experiments was measured by averaging values obtained at all time points during baseline periods. These periods were defined as the time span from 30 to 40 sec after the end of each stimulus. For each ROI, differences in resting CBF between groups were tested using the Wilcoxon nonparametric rank-sum test.

### Modeling and analysis of functional hyperemia

For analysis of functional hyperemia (i.e., local blood flow responses to neural activation within motor or visual cortex areas), CBF data were first normalized to the mean resting CBF value obtained in each subject (percentage increase from baseline). Thereafter, the average CBF increase measured over the entire stimulation period (sum of all stimulation blocks) was compared between patients and controls using the Wilcoxon nonparametric rank-sum test.

For further analysis of blood flow responses, functional hyperemia dynamics was compared between patients and controls using a piecewise linear mixed-effects model, and CBF values were measured during the full activation periods; values obtained during the first 5 sec of stimulation were discarded. This time-dependent model, which allowed investigation of changes in blood flow responses over different lengths of stimulation, is expressed as $y_n(t,k,a) = m(t,k,a) + g(t,k,a).\phi_n + U_n + R_n$, where

- $y_n$ summarizes data variations in the $n^{th}$ subject as the sum of $m(t,k,a)$, a function modeling CBF changes during the different stimulation periods in each experiment, and g($t$, $k$, $a$), a function modeling the difference in changes between patients and controls over the entire course of the experiment according to time ($t$) to stimulation sequence number $k$ (relatively to the start of stimulation inside each stimulation block) and the age of the subject $a$ (where $a$ is between −15 and 15 and equals 0 for age = 45 years);
- $m(t,k,a) = \beta_0 + k.\beta_1 + a.\beta_2 + \sum_{i=1}^{N_p}\left[v_i(t-t_i)^+\right]$, in which $\beta_0$, $\beta_1$, and $\beta_2$ correspond to the initial CBF value, the hypothetical baseline blood flow variation along multiple repeated sequences and the effects of age on blood flow variations, respectively, and $t_i$ represents the lower bounds of $N_p$ in 5-sec segments during the different stimulation periods (for 20-sec blocks: $N_p$ = 3 segments and $t_i = \{5, 10, 15\}$ seconds; for 40-sec blocks, $N_p$ = 7 segments and $t_i = \{5, 10, 15, 20, 25, 30, 35\}$ seconds; for the decrease between 15 and 35 sec: $N_p$ = 1 segment and $t_1$ = 15), and where $v_i$ models functional hyperemia dynamics in general;
- $g(t,k,a) = \gamma_0 + k.\gamma_1 + a.\gamma_2 + \sum_{i=1}^{N_p}\left[\xi_i(t-t_i)^+\right]$, in which $\gamma_0$, $\gamma_1$, and $\gamma_2$ corresponds to the initial CBF difference between patients and controls, the difference in CBF changes after repeated MRI sequences and the difference between groups of CBF variations related to the age effect, respectively, and where $\xi_i$ models the hypothetic difference in hyperemia dynamics between patients and controls;
- $\varphi_n$ is a binary independent variable equal to 1 for all patients and 0 for all controls;
- $U_n$ corresponds to the random effect for inter-subject baseline variability, where $U_n \sim \mathcal{N}(0, \sigma_U^2)$;
- $R_n$ corresponds to the residual error of each measure, where $R_n \sim \mathcal{N}(0, \sigma_R^2)$.

The difference in the dynamics of CBF changes over time was used to test quantitative differences between controls and patients without a priori assumptions (except the choice of $t_i$) using the maximum likelihood estimation method. Any subject with a Cook's distance value greater than 1 was assigned the first position,[21] after which the likelihood ratio of the model, including those including one or several tested parameters versus a model that does not include these parameters, was calculated for testing different hypotheses. The analysis was performed using R Studio software with the "influence.ME" package for computation of Cook's distance and the "lme4" package for fitting linear mixed-effects models.[22]

## EEG analysis

### Preprocessing

Gradient/pulse and ballistocardiogram artifacts were first corrected using the average artifact suppression (AAS) method implemented in BrainVision Analyzer2 software,[23] with application of an artifact waveform template

 

of 5520 msec (2TR) averaged on a sliding window over 31 artifact repetitions. Signals were also filtered (low pass at 30 Hz with band rejection at 18 Hz) to suppress the remaining main and harmonic gradient frequencies. The signals were then down-sampled at 250 Hz. Ballistocardiogram artifacts were corrected using an artifact waveform template averaged on a sliding window over 21 cardiac cycles, assessed visually in the ECG channel. Eyeblink artifacts were automatically suppressed using an independent components analysis implemented in the Fieldtrip toolbox for MATLAB.[24] Independent components were calculated from EEG sensors (Infomax algorithm) and correlated with the frontopolar EEG electrode with the lowest impedance between Fp1 and Fp2. The component with the highest correlation was then suppressed when reconstructing EEG signals from all components.

### Extraction of visual evoked potentials

The electrical visual response during the flickering checkerboard stimulation was evaluated based on the amplitude of the P100 wave extracted from the EEG signal obtained through the occipital EEG electrodes. P100 wave is a neural response that occurs around the calcarine fissure in response to a strong contrast change in the visual field.[25–28] The signals of the three medial occipital channels, O1, Oz, and O2, were averaged to obtain a single signal representative of primary visual cortex activity. For each scan of each subject, all responses evoked by individual checkerboard reversals were averaged to obtain the average latency of the P100 wave. The P100 amplitude was then calculated for each subject as the mean amplitude of each visual evoked potential (VEP) around the average latency ($\pm$ 5 ms).

### Modeling and analysis of P100 amplitude

To evaluate possible alterations of the P100 wave amplitude, we applied the piecewise linear mixed-model as used for blood flow analysis and described above, but where $y_n(t,k,a)$ is the P100 wave amplitude of the $n^{th}$ subject.

## Results

### Study design

A total of 19 CADASIL patients (11 females, eight males) and 19 control subjects (12 females, 7 males) were initially included in the study, which followed the protocol detailed in Figure 1. Mean age was 43.6 $\pm$ 6.7 years (range, 33–57 years) in patients and 43.2 $\pm$ 8.0 years (range, 30–58 years) in controls; all subjects but one, were right-handed. Rankin score at the time of MRI was 1 in eleven patients and 0 in the others; all control subjects had a Rankin score of 0. All patients presented with confluent white-matter hyperintensities on FLAIR (fluid attenuation inversion recovery) images, but showed no visually detectable regional or global cerebral atrophy on 3D-T1 images. Fifteen patients lacked lacunes, and four had from 1 to 3 lacunes. Microbleeds were absent except in one individual, who had two microbleeds. These signal abnormalities were absent in all healthy individuals.

Subjects performed a simple motor task with their nondirective hand that was visually cued by a flickering checkerboard (Fig. 1A and B) while undergoing an ASL sequence with simultaneous EEG recording (Fig. 1C). Activated voxels were detected individually in all subjects using a specific automatic method (Fig. 1D). Voxels that showed significant activation in response to visual stimulations were detected within the primary visual cortex, around and above the calcarine fissure, in all subjects (Fig. 2A). The size of visual regions of interest (ROI) was 70.5 $\pm$ 18.9 voxels (range, 36–100) in the patient group and 67.3 $\pm$ 25.1 voxels (range, 29–105) in the control group ($P = 0.664$, Student's test). Motor cortex activity was always detected in the contralateral hemisphere (Fig. 2B). In each case, the ROI observed around the central sulcus included a part of the primary motor cortex area and spread posteriorly to the central sulcus in the somatosensory area. The mean size of motor ROIs was 25.9 $\pm$ 9.1 voxels (range, 9–49) in patients and 28.6 $\pm$ 13.8 voxels (range, 3–60) in controls ($P = 0.484$).

### Comparison of mean variations in CBF between patients and controls over 20- and 40-sec stimulations in visual and sensorimotor cortexes

Resting CBF did not differ between patients and controls in the visual (56.5 $\pm$ 20.5 and 54 $\pm$ 13.5 mL/100 g/min, respectively) or motor (52.8 $\pm$ 19.2 and 53.3 $\pm$ 15.8 mL/100 g/min, respectively) cortex ($P = 0.587$). Changes in CBF in response to stimulations were calculated only in visual and motor ROIs. The mean increases in CBF over 20- and 40-sec stimulations in visual and sensorimotor cortexes are shown in Figure 2C and D. Although there was a trend toward diminished functional hyperemia in patients compared with control subjects over 20-sec stimulation blocks, these differences did not reach statistical significance (visual, $P = 0.151$; motor, $P = 0.181$). During 40-sec stimulations, a small, but significant, reduction in the blood flow response was observed in

 

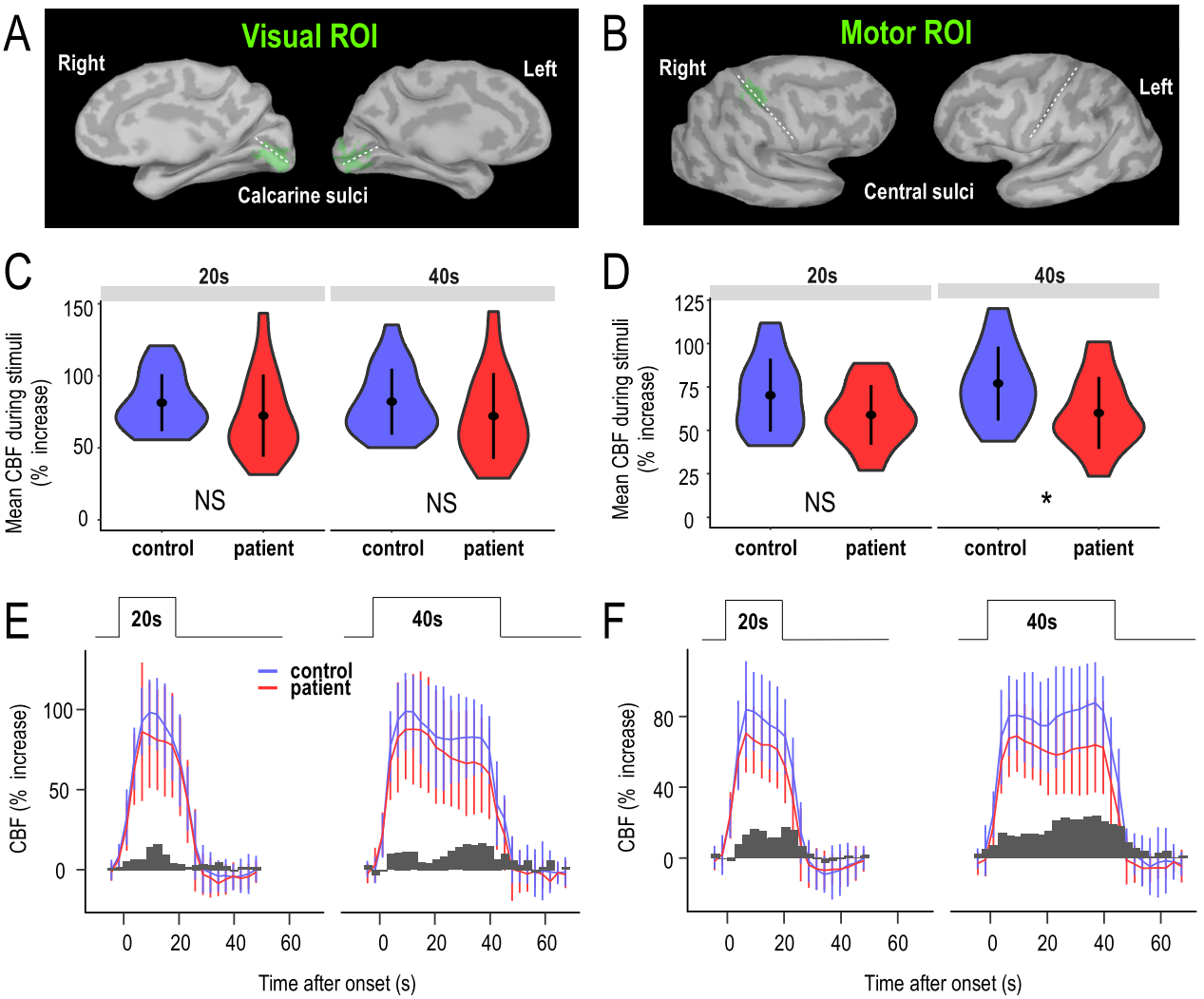


**Figure 2.** Mean amplitude of functional hyperemia in visual and motor cortexes. (A and B) ROIs projected on the surface of the primary visual cortex and motor (hand) cortex (B) in a representative control subject. The ROI selected is shown in green, and calcarine and central sulci are marked by white dashed lines. (C and D) Average increase in CBF during 20- and 40-sec stimulations in visual (C) and motor (D) ROIs are presented as violin plots for controls and patients, where points and lines represent means and standard deviations, respectively, and the width represents the frequency of data at different values. (E and F) Time series of functional hyperemia during 20- and 40-sec stimulations in visual ROIs (E) and motor ROIs (F). Error bars represent standard deviations between subjects in each group. Dark gray bars represent the observed differences between mean values in control subjects and patients over each time frame.

motor ROIs ($P = 0.027$), but not in visual ROIs ($P = 0.189$).

## Analysis of functional hyperemia dynamics over 20- and 40-sec stimulations in visual and sensorimotor cortexes using a piecewise linear mixed-effects model

Despite the small difference in mean CBF change and large variability of CBF values measured during the experiment, we noted that the largest differences between patients and controls occurred predominately after 20 sec in both the visual and motor cortex (Fig. 2E and F, see bar plots of differences vs. time). Thus, we hypothesized that the dynamics, rather than the amplitude, of CBF increases in response to motor or visual stimulation was particularly altered in CADASIL. To analyze the dynamics of blood flow responses in patients and controls in a time-independent manner, we built a piecewise, linear mixed-effects model to fit functional hyperemia. In this model, the dynamics of the blood flow response was defined as the slopes over successive 5-sec time segments

 

(the limit of the time resolution of our recordings). Various potential nondynamic effects on mean CBF measures due to age, the number of MRI sequences or inter-subject variability (modeled as a random effect) were thus considered with no other assumptions regarding the intrinsic dynamics of data aside from time sampling (Figure 3).

This analysis, which focused on changes detected during activation periods from the initial CBF rise (assumed to be complete 5 sec after stimulation onset) to the end of neural stimulation, showed that functional hyperemia dynamics differed between patients and controls (Table 1). This difference was significant in both visual ($P = 0.000736$, likelihood-ratio test) and motor ($P = 0.000001$) ROIs over 40-sec stimulation periods but not over 20 sec (Fig. 3A and B and Table 1). Blood flow responses related to the repetition of motor-stimulation sequences over 40 sec also significantly decreased in patients ($P = 0.0011$), but no such decrease was detected for long (40 sec) visual stimulations.

## Comparison of the slopes of functional hyperemic responses in sensorimotor and visual cortexes over the 15–30-sec time frame between patients and controls

An analysis of the time course of functional hyperemic responses during 40-sec stimulations in both motor and visual ROIs showed a decrease in the CBF response in patients during the second half of the stimulation period (Fig. 3A and B). This difference increased after 15 sec in both visual and motor ROIs (Fig. 3A and B, histograms). The decrease in the CBF response was analyzed by comparing the slopes of a simple, single-segment linear-regression model applied to CBF values between 15 and 30 sec after the stimulus onset (Fig. 3A and B, yellow time segment), considered as a single 15-sec segment in Figure 4 (segment with minimal *P* value). Slopes calculated in patients and control groups were significantly different in both visual ($P = 0.00723$) and motor ($P = 0.000907$) ROIs.

## Analysis of P100 waves from simultaneous evoked potentials obtained with 20- and 40-sec visual stimulations

The neural response evoked by visual stimulations was assessed in parallel with measures of evoked potentials and the amplitude of their derived P100 waves, which are known to originate from the calcarine fissure (Fig. 3C and D). The average amplitude of P100 measured over 20 sec after each visual contrast reversal did not differ between patients ($1.7 \pm 2.3$ $\mu$V) and controls ($1.9 \pm 2.1$ $\mu$V; $P = 0.65$; Wilcoxon signed-rank test); peak delay was also not significantly different between patients ($0.108 \pm 0.013$ sec) and controls ($0.109 \pm 0.0094$ sec; $P = 0.73$). Similarly, patients and controls showed no differences in average amplitude ($2.52 \pm 1.51$ vs. $2.39 \pm 1.22$ $\mu$V; $P = 0.81$) or peak delay ($0.110 \pm 0.013$ vs. $0.110 \pm 0.009$ sec; $P = 0.9$) over 40 sec (Fig. 3C). Using the piecewise linear mixed-effects model based on successive 5-sec time frames used previously for analyzing CBF values, we found no significant difference in the dynamics of P100 waves between patient and control groups for either 20-sec ($P = 0.329$) or 40-sec ($P = 0.905$) stimulations (Fig. 3D). A comparison of the slopes of P100 responses derived from EEG records in the visual cortex over the 15–30-sec time segment, as was previously done for CBF values in the simplified model, show no significant difference ($P = 0.928$) (Fig. 4).

## Analysis of the slope of functional hyperemic responses limited to the 15–30-sec time frame in a replication sample and data obtained in the full sample

We hypothesized that the slope of the functional hyperemic response could be a biomarker of NVC alterations at an early stage of CADASIL. To test the replicability of the slope difference between patients and controls over the 15–30-sec time frame, we analyzed a separate sample of 10 CADASIL patients (mean age, $47.4 \pm 3.5$ years; range, 42–53 years; male/female ratio = 6/4) and 10 age-matched healthy subjects (mean age, $47.5 \pm 5.1$ years; range: 41–56 years, male/female ratio = 3/7) using selection criteria identical to those for the initial study population. A similar, but shorter, experimental paradigm composed of only four stimulation sequences was used for these analyses; data were subsequently processed as described for the more complex paradigm. Visual ROIs comprised $67.4 \pm 19.7$ voxels (range, 32–95) in patients and $77.7 \pm 16.0$ voxels (range, 62–102) in age-matched controls. With visual stimulations over 40 sec, the slope of the functional hyperemic response between 15 and 30 sec was lower in CADASIL patients (−24.4%) than in healthy subjects (−5.2%, $P = 0.0238$) (Fig. 4 and Table 2). The size of motor ROIs was $17.6 \pm 11.5$ voxels (range, 6–37) in patients and $23.6 \pm 15.4$ voxels (range, 2–55) in controls, values that are smaller than those obtained in the initial sample. With a 40-sec motor stimulation, the hyperemic response between 15 and 30 sec in the sensorimotor cortex decreased in patients (-11.9%), but increased in controls (+ 8.9%, $P = 0.0254$) (Fig. 4 and Table 2). In this additional sample, neural activity, measured using P100 amplitudes, did not differ between patients and controls ($P = 0.944$) (Fig. 4). An analysis performed as previously but using data from the entire sample of patients and controls ($n = 58$) showed that the

 

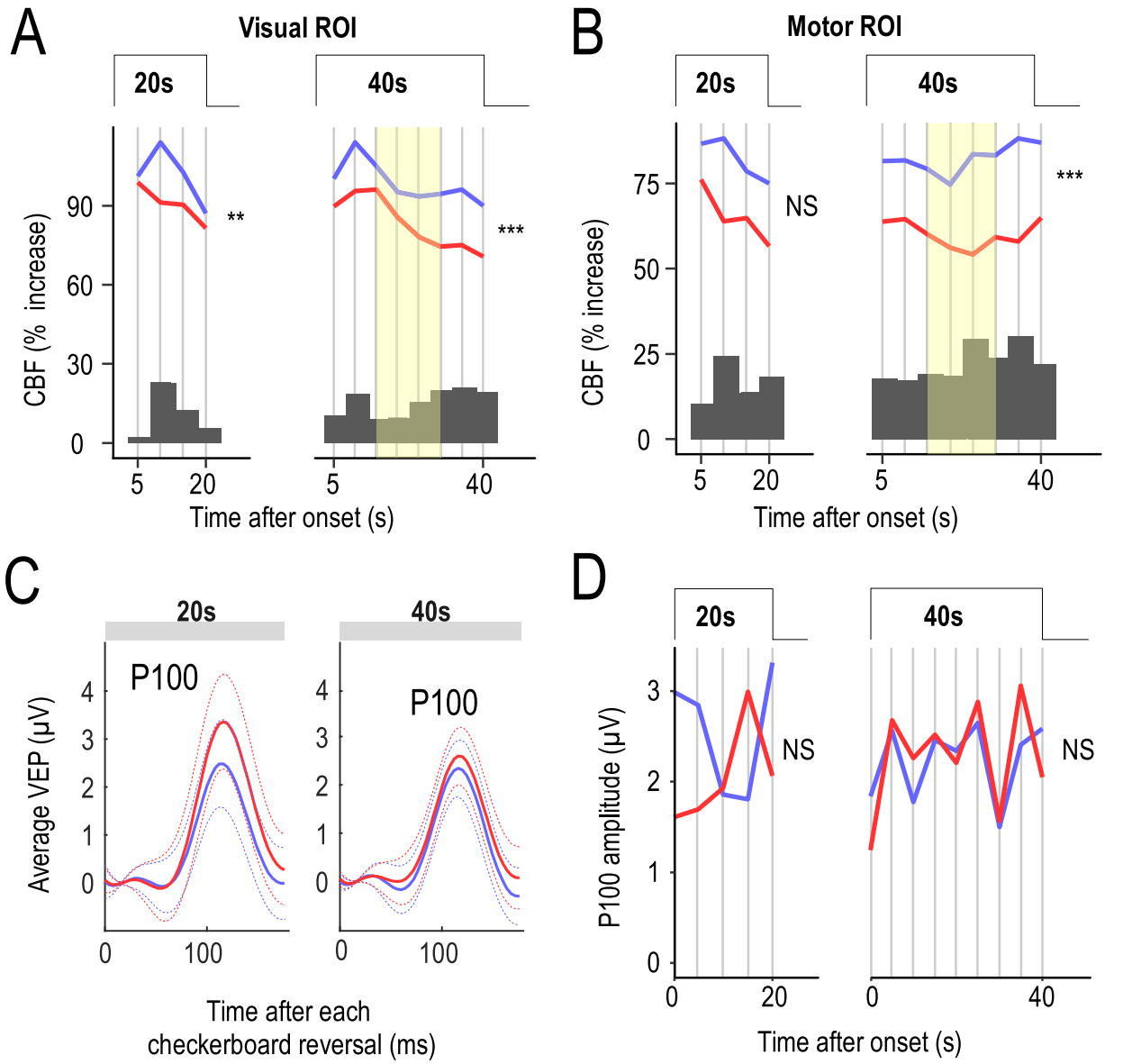


**Figure 3.** Analysis of functional hyperemia dynamics and P100 waves during neural tasks. (A and B) Functional hyperemia in the visual cortex (A) and sensorimotor cortex (B) during activation (after an initial 5-sec period of rapid increase) was fitted using a piecewise (succession of 5-sec steps) linear mixed-effects model in 19 patients and 19 controls. Likelihood ratio tests showed a significant difference in the dynamics (slopes) of the response between patients (red) and controls (blue) that was larger at the end phase of the stimulation period for long-lasting stimulations (**$P < 0.01$, ***$P < 0.001$). Changes in functional hyperemia dynamics were mainly detected between 15 and 30 sec (yellow). Dark gray bars represent the difference between mean CBF values measured at different time intervals in control subjects and patients. (C) Average values (solid line) of evoked potentials (shown with their standard deviation, dotted line) obtained after each visual reversal stimulation did not differ between the two groups. (D) Analysis of P100 waves over 5-sec segments using the piecewise linear mixed-effects model showed no significant difference over the entire duration of stimulation between the two groups.

slope of the linear regression based on CBF values measured between 15 and 30 sec also differed between the two groups in both visual ($P = 0.00000046$) and motor ($P = 0.0000012$) ROIs (Table 2). Finally, the complete piecewise model was also fitted to the full dataset (Fig. 5 and Table 3). This analysis confirmed a difference in functional hyperemia dynamics that remained highly significant in response to 40-sec stimulations (visual, $P = 1.28 \times 10^{-5}$; motor, $P = 1.18 \times 10^{-6}$), but not to 20-sec stimulations (visual, $P = 0.133$; motor, $P = 0.431$).

 

**Table 1.** Summary of group effects tested using a piecewise linear mixed-effects model in 19 patients and 19 age-matched controls (initial sample).

| | | Visual | | | | Motor | | | |
|---|---|---|---|---|---|---|---|---|---|
| Effect | Df | Est. | SE | $\chi^2$ | *P*-value | Est. | SE | $\chi^2$ | *P*-value |
| 20-s CBF increase (%) | | | | | | | | | |
| Group (global) | 6 | / | / | 16.59 | 0.0109 | / | / | 11.46 | 0.0753 |
| Group: Age | 1 | −1.546 | 1.302 | 1.384 | 0.2395 | −1.113 | 0.993 | 1.234 | 0.2666 |
| Group: Sequence | 1 | 0.257 | 0.846 | 0.092 | 0.7614 | 0.837 | 0.793 | 1.116 | 0.2908 |
| Group: Dynamics | 3 | / | / | 14.09 | 0.0028 | / | / | 5.746 | 0.1246 |
| 40-s CBF increase (%) | | | | | | | | | |
| Group (global) | 10 | / | / | 30.41 | 0.0007 | / | / | 46.87 | 1E-06 |
| Group: Age | 1 | −1.572 | 1.323 | 1.385 | 0.2393 | −1.222 | 1.034 | 1.37 | 0.2419 |
| Group: Sequence | 1 | 0.812 | 0.496 | 2.68 | 0.1016 | 1.665 | 0.508 | 10.71 | 0.0011 |
| Group: Dynamics | 7 | / | / | 25.08 | 0.0007 | / | / | 29.33 | 0.0001 |
| 20-s P100 amplitude (μV) | | | | | | | | | |
| Group (global) | 7 | / | / | 5.924 | 0.5486 | | | | |
| Group: Age | 1 | −0.087 | 0.097 | 0.804 | 0.37 | | | | |
| Group: Sequence | 1 | 0.15 | 0.233 | 0.41 | 0.5217 | | | | |
| Group: Dynamics | 4 | / | / | 4.614 | 0.3292 | | | | |
| 40-s P100 amplitude (μV) | | | | | | | | | |
| Group (global) | 11 | / | / | 3.882 | 0.9733 | | | | |
| Group: Age | 1 | −0.037 | 0.065 | 0.325 | 0.5688 | | | | |
| Group: Sequence | 1 | −0.002 | 0.084 | 4E-04 | 0.9848 | | | | |
| Group: Dynamics | 8 | / | / | 3.421 | 0.9052 | | | | |

CBF variations measured during 20- and 40-sec activations of the visual and sensorimotor cortex were tested. P100 amplitude in the visual cortex in response to 20- and 40-sec visual stimulations were also tested. Df, degree of freedom. Estimated values (Est.) are only provided for effects related to a single parameter (i.e., Df = 1). Red values indicate *P*-values less than 5% based on likelihood ratio tests.

## Discussion

In this study, we detected significant alterations in NVC at an early stage of CADASIL using ASL-fMRI in combination with EEG. These results were obtained in patients with a mean age of about 43 years, long before the occurrence of disability and cognitive decline that develop with cerebral atrophy at the latest stage of the disease.[3] Alterations in functional hyperemia were detected with both visual and motor stimulations, but only with longer (40 sec) stimulations. A specific mathematical model showed major changes in functional hyperemia dynamics in patients, manifesting as a decrease in blood flow response after a delay of at least 15 sec. With inclusion of additional data from a replication sample, the slope of blood flow curves between 15 and 30 sec emerged as a potential biomarker of NVC dysfunction at an early stage of the disease.

An assessment of mean changes in absolute CBF values over 20 or 40 sec of visual or motor stimulation revealed a significant decrease in functional hyperemia in CADASIL patients only for long-lasting motor tasks. Resting CBF values in these patients were in the normal range, as previously reported in the cortex at the onset of the disease.[29] These results were obtained despite the large intersubject variability of CBF measures over the cortex and the use of variable-sized ROIs, selected from stimulus-based maps. To assess hyperemia response dynamics, we developed a specific mathematical model that allowed analysis of functional hyperemic responses over successive 5-sec time frames during stimulation periods while accounting for potential effects of age or the repetition of tasks throughout the duration of experiment. Applying this model, we found that the dynamics of blood flow responses differed substantially between patients and healthy individuals. This difference was highly significant for both repeated visual and motor tasks, but only for 40-sec stimulations. Notably, this decrease in functional hyperemia was detected after a delay of 15 to 20 sec in the patient group, both in the visual and sensorimotor cortex. Thus, the decline in hemodynamic responses across repetitive motor-stimulation sequences in the patient group revealed by the statistical model cannot account for the differences in hemodynamics. Moreover, this effect was not detected for long-lasting visual stimulations. Additional investigations are needed to determine whether these effects in patients might be explained by a greater fatigue factor associated with repeated hand movements over a long time compared with less demanding visual stimulations.

To assess neural activity using an independent approach, we obtained EEG recordings from patients

 

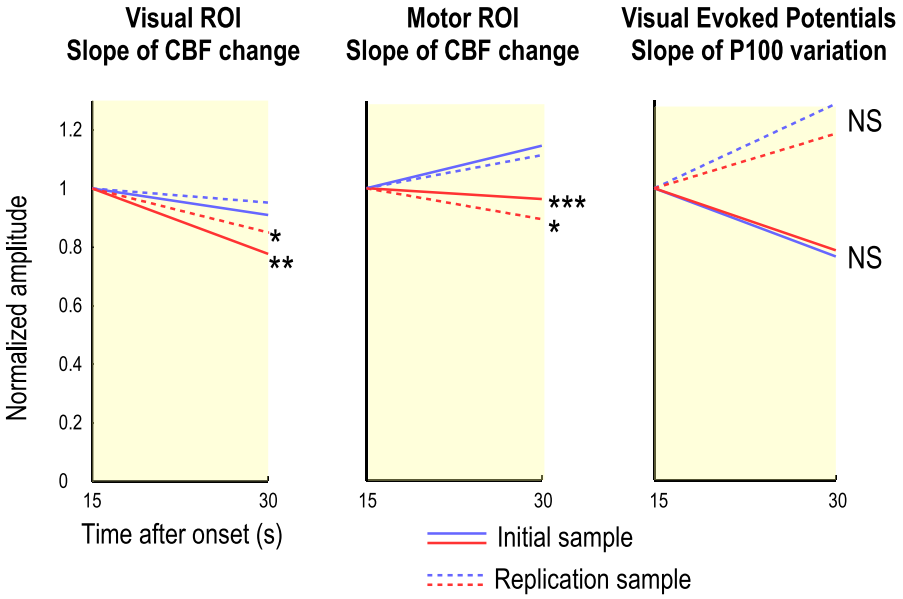


**Figure 4.** Slope of functional hyperemia over the 15–30-sec time frame in patients and controls. An analysis of the CBF response, performed by comparing the slopes between 15 sec and 30 sec (yellow segment in figure 3) after the stimulus onset using a simple single-segment linear regression model, showed a significant difference between 19 patients and 19 controls in visual ($P = 0.00723$) and motor ($P = 0.000907$) ROIs. Similar results were obtained in an analysis of a replication sample of 10 patients and 10 additional healthy individuals. Conversely, results obtained using the same analysis of P100 amplitudes derived from EEG records in the visual cortex showed no significant difference between the two groups ($P = 0.928$). *$P < 0.05$; **$P < 0.01$; ***$P < 0.001$

**Table 2.** Estimation and likelihood ratio test of the slope of the decrease in the functional hyperemic response between 15 and 30 sec after stimulus onset.

| | Visual | | | | Motor | | | |
|---|---|---|---|---|---|---|---|---|
| Sample | Est. | SE | $\chi^2$ | *P*-value | Est. | SE | $\chi^2$ | *P*-value |
| CBF (% of baseline) | | | | | | | | |
| Initial ($n = 38$) | −12.26 | 4.56 | 7.214 | 0.00723 | −14.52 | 4.371 | 11.01 | 0.00091 |
| Replication ($n = 20$) | −19.19 | 8.474 | 5.111 | 0.02377 | −20.78 | 9.284 | 4.997 | 0.0254 |
| Whole ($n = 58$) | −14.03 | 4.03 | 12.1 | 0.0005 | −16.03 | 4.05 | 15.63 | 7.7E-05 |
| P100 amplitude (μV) | | | | | | | | |
| Original ($n = 38$) | 0.072 | 0.8 | 0.008 | 0.92837 | | | | |
| Validation ($n = 20$) | −0.087 | 1.242 | 0.005 | 0.94431 | | | | |
| Whole ($n = 58$) | 0.035 | 0.687 | 0.003 | 0.9591 | | | | |

Results obtained in the initial sample (19 patients and age-matched controls) in a replication sample of 10 patients and age-matched controls, and in the whole sample (29 patients and 29 age-matched controls) are presented. Red values indicate *P*-values less than 5% based on likelihood ratio tests.
Est., estimated values.

inside the MRI scanner during each visual stimulation period. Our analysis of evoked potentials at the peak which occurred after each visual contrast reversal (P100), revealed no significant differences between patients and healthy individuals with 20- or 40-sec visual tasks, a result in line with a previous report based on three CADASIL cases.[30] Both the average amplitude and delay to the peak were statistically indistinguishable between the two groups. Moreover, an analysis of changes in P100 over successive 5-sec time frames using our piecewise linear mixed-effects model showed no significant change in P100 waves, regardless of the duration of visual stimulation. Since the P100 wave originates from the calcarine fissure, where the largest changes in blood flow are also detected during visual stimulations,[25–28] our findings support the conclusion that the altered dynamics of blood flow responses during neural tasks in patients is not related to a reduction in the neural response, but may

 

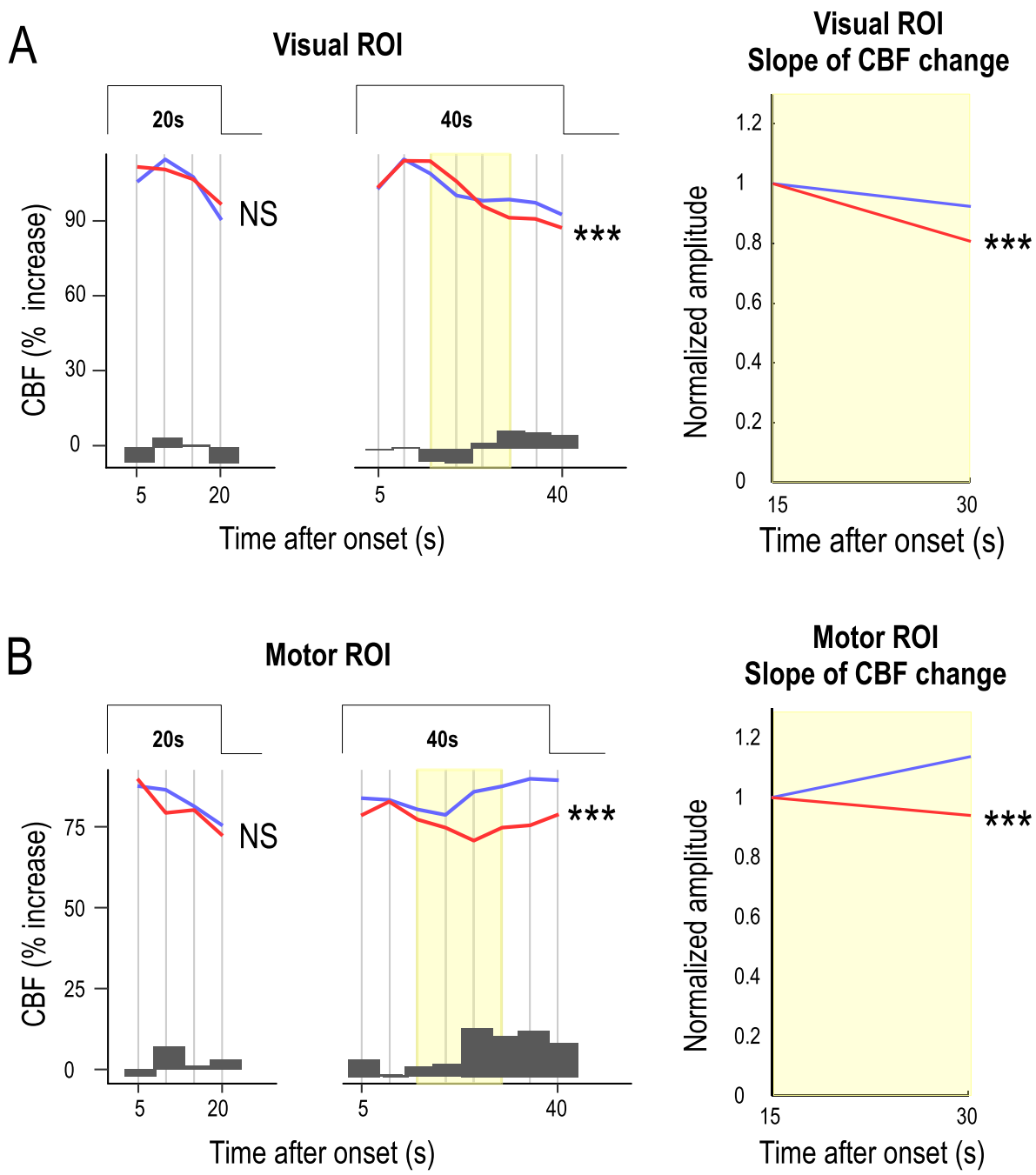


**Figure 5.** Functional hyperemic responses in the entire population. (A and B) Functional hyperemia in the visual cortex (A) and sensorimotor cortex (B) during activation was fitted in the whole population (29 patients and 29 controls) as was previously done using the piecewise linear mixed-effects model. Likelihood ratio tests showed a significant difference between the dynamics (slopes) of the response obtained in patients (red) and controls (blue) for long-lasting stimulations (***$P < 0.001$). Changes in functional hyperemia dynamics appeared between 15 and 30 sec (yellow). Dark gray bars represent differences between mean CBF values measured at the different time intervals in control subjects and patients. The CBF response analyzed by comparing the slopes between 15 and 30 sec after the stimulus onset using a simple, single-segment linear-regression model confirmed the highly significant difference between the 29 patients and 29 controls.

rather reflect a decrease in NVC efficiency originating from the vascular bed in the context of neural stimulations that extend over time.

Based on these findings, we hypothesized that the altered NVC dynamics observed in CADASIL patients might reflect early dysfunction of the cerebral microvasculature

 

**Table 3.** Summary of group effects tested using a piecewise linear mixed-effects model in the whole sample of 29 patients and 29 age-matched controls.

| | | Visual | | | | Motor | | | |
|---|---|---|---|---|---|---|---|---|---|
| Effect | Df | Est. | SE | $\chi^2$ | *P*-value | Est. | SE | $\chi^2$ | *P*-value |
| 20s CBF increase | | | | | | | | | |
| Group (global) | 6 | / | / | 6.781 | 0.3416 | / | / | 3.522 | 0.7411 |
| Group: Age | 1 | −1.273 | 1.27 | 0.995 | 0.3185 | −0.449 | 1.047 | 0.183 | 0.6684 |
| Group: Sequence | 1 | −0.386 | 0.809 | 0.228 | 0.6329 | 0.557 | 0.781 | 0.508 | 0.476 |
| Group: Dynamics | 3 | / | / | 5.603 | 0.1326 | / | / | 2.755 | 0.4309 |
| 40s CBF increase | | | | | | | | | |
| Group (global) | 10 | / | / | 35.88 | 9E-05 | / | / | 47.61 | 7E-07 |
| Group: Age | 1 | −1.288 | 1.337 | 0.92 | 0.3375 | −0.358 | 1.091 | 0.107 | 0.7432 |
| Group: Sequence | 1 | 0.247 | 0.479 | 0.266 | 0.606 | 1.332 | 0.509 | 6.832 | 0.009 |
| Group: Dynamics | 7 | / | / | 34.68 | 1E-05 | / | / | 40.15 | 1E-06 |
| 20s P100 amplitude | | | | | | | | | |
| Group (global) | 7 | / | / | 5.851 | 0.5572 | | | | |
| Group: Age | 1 | −0.118 | 0.098 | 1.428 | 0.232 | | | | |
| Group: Sequence | 1 | −0.039 | 0.183 | 0.046 | 0.831 | | | | |
| Group: Dynamics | 4 | / | / | 4.253 | 0.3729 | | | | |
| 40s P100 amplitude | | | | | | | | | |
| Group (global) | 11 | / | / | 6.522 | 0.8364 | | | | |
| Group: Age | 1 | −0.073 | 0.068 | 1.132 | 0.2874 | | | | |
| Group: Sequence | 1 | 0.013 | 0.076 | 0.028 | 0.8676 | | | | |
| Group: Dynamics | 8 | / | / | 5.175 | 0.7388 | | | | |

CBF during 20- and 40-sec activation of visual and motor cortex was tested. P100 amplitude in the visual cortex in response to 20- and 40-sec visual stimulations were also tested. Df, degree of freedom. Estimated values (Est.) are only provided for effects related to a single parameter (i.e., Df = 1). Red values indicate *P*-values less than 5% based on likelihood ratio tests.

at the onset of the disease, and as such could be translated into a potential biomarker in future studies. A simplified analysis in which the linear slope of functional hyperemia was calculated over a single time frame from 15 to 30 sec during stimulation periods rather than over 5-sec steps not only confirmed these results in the original sample of 19 patients and 19 controls, but also in a replication sample of 10 additional patients and 10 age-matched controls. Moreover, a parallel analysis of P100 waves from visual evoked potentials over the same time frame showed no difference between the two groups in either the initial or replication samples. Finally, and as expected, in the whole population (29 patients and 29 controls), considering functional hyperemia over 15–30 sec as a single marker confirmed a strong and highly significant difference between the two groups. While no marker of vascular dysfunction that affects primarily smooth muscle cells and pericytes has yet been identified in CADASIL, these data suggest that a measure as simple as the slope of the blood flow response obtained with fMRI over a single, delayed time frame represents a promising biomarker of early microvascular dysfunction in CADASIL. Additional investigations are now needed to determine whether and how this measure could be made sufficiently robust and sensitive to assess disease progression and clinical severity.

Studies have consistently reported a significant reduction in the amplitude of the CBF response in CADASIL mouse models. For example, CBF increases in the somatosensory cortex elicited by repeated whisker stimulations over 60 sec were reported to be reduced by 30% in these mice.[7] Notably, these results were obtained from mice that were 6 months old, simultaneously to the appearance of cerebral tissue lesions.[6,31] Accumulation of TIMP3 (tissue inhibitor of metalloproteinases-3), a component of the extracellular matrix in the wall of microvessels, was recently shown to disrupt signaling of the matrix metalloproteinase, ADAM17, resulting in an increase in the number of voltage-dependent potassium channels at the membrane surface of smooth muscle cells.[6,8] These early changes likely contribute to the reduced response to neural stimuli in CADASIL model mice.[6] In this study performed in CADASIL patients, all of whom were all at early stage of the disease but showed white-matter lesions on MRI, functional hyperemia dynamics were found to be altered at the late phase of long stimulations, whereas the amplitudes of responses were not different or only differed slightly between patients and healthy individuals. The contrast between these findings and preclinical results might be explained by large differences in experimental conditions, stimuli, time scales, signals produced, and

 

underlying neurophysiological characteristics. We also cannot exclude the possibility that the much larger variability of CBF measures obtained using ASL-fMRI techniques in humans precluded the detection of modest differences in local CBF changes between patients and controls. Our innovative approach using a dedicated model for analyzing blood flow response-time curves in humans might have been particularly helpful in avoiding this pitfall by focusing on early changes in the shape of the response curve that are identifiable long before the decrease in amplitude becomes significant. Alternatively, it is conceivable that the reductions in blood flow responses in CADASIL patients detected with long stimulations are related to mechanisms that are specifically involved at a particular stage of the NVC process. Accumulating evidence indicates that NVC is initially composed of a fast, phasic component that reflects a hyperpolarizing wave initiated in capillary endothelial cells that rapidly back-propagates along the ascendant vascular tree to arteriolar smooth muscle cells.[32] This process may also be accompanied by direct hyperpolarization of smooth muscle cells by activated astrocytes.[33] By contrast, the mechanisms involved in sustaining the hemodynamic response during prolonged neural stimulation are not fully understood, although recent data suggest that a significant proportion of astrocytes that were not previously involved are progressively recruited into action by the release of glutamate from neurons within several seconds of the stimulation onset.[34–36] Alterations in communication and signaling secondary to NOTCH3-ECD accumulation between astrocytic endfeet and vascular smooth muscle cells or pericytes[37] might thus be an additional contributor to the decreased efficiency of NVC with long neural stimulations.

This is the first report of precise CBF measures obtained in vivo using ASL, which showed that functional hyperemia dynamics are altered early in patients with ischemic cerebral SVDs. In a previous, small fMRI study of five CADASIL patients with a mean age of 55 years, the BOLD response stimulated in cortical areas was found to be within the normal limits, but functional hyperemia dynamics was not specifically evaluated.[38] Previous fMRI data obtained using BOLD contrast in patients with probable cerebral amyloid angiopathy, who sometimes had severe clinical manifestations and cerebral hemorrhages, also cannot be compared with the present results.[39] Despite the lack of a large prestimulus sequence for measuring resting CBF, a potential contribution of chronic hypoperfusion to the alterations observed appear also unlikely since resting CBF during the sampling did not differ between patients and controls and because alterations of functional hyperemia dynamics were detected in the model independently of resting CBF measures. There are multiple strengths of our study. Patients were selected according to strict criteria; data were analyzed by mathematical modeling, allowing an independent evaluation of CBF dynamics along each task; measures were obtained in two different cortical areas using two different durations of stimulation; and results obtained in an initial group of patients were replicated in an independent sample. The limitations include the small spectrum of clinical manifestations, which prevented an analysis of clinical correlates; the variability of raw data, which reduced our ability to analyze results at the individual level; and the relative complexity of data processing pipelines and modeling.

In conclusion, this study shows that NVC dynamics, which can be assessed in vivo using ASL-fMRI and long neural stimulations, is altered at the early stage of CADASIL. A late decrease in the cortical hyperemic response can be assessed using a simple marker calculated over a limited time-frame during 40-sec neural stimulations. Additional studies are warranted to determine how these functional alterations evolve over time, correlate with disease severity, and can be used to monitor the progression of microvascular changes and treatment effects.

## Acknowledgments

We acknowledge all patients who participated in this research, their families, and the association CADASIL France for their active collaboration. Patients were recruited with the help of Solange Hello, Jocelyne Ruffie, and Abbas Taleb from the referral Centre CERVCO and ARNEVA (Association de Recherche en Neurologie Vasculaire). Dr Herve collected data which were crucial for the initial selection of patients. We warmly thank Pr Chevret for her statistically sound advice. This study was supported by grants from the Fondation Leducq (Transatlantic Network of Excellence on the Pathogenesis of Small Vessel Disease of the Brain; http://www.fondationleducq.org), ANR (Ministry of Health and Research, (Commissariat General à l'Investissement) RHU TRT_cSVD). Clement Huneau was funded successively by Fondation de l'Avenir and by the Leducq Foundation.

## Conflict of Interest

CH, HB and HC have filed a Patent Application (deposit No. 17305045.1 (Neurovascular coupling studied using fMRI and EEG); the other authors declared no competing interests.

## Author Contribution

Clément Huneau participated to the acquisition of data and analyzed the results obtained. He also wrote the first

 

draft of the manuscript. Marion Houot participated to the analysis of data. Benoit Béranger was involved in the acquisition of data and control quality. Christian Giroux included all patients in the study and selected healthy individuals, he participated to the clinical and imaging examination of all subjects. Habib Benali and Hugues Chabriat were responsible for the conception of the study and participated in the writing of the manuscript together with A Joutel and Clement Huneau.

## References


1. Longden TA, Hill-Eubanks DC, Nelson MT. Ion channel networks in the control of cerebral blood flow. J Cereb Blood Flow Metab 2016;36:492–512.
2. Iadecola C. The Neurovascular Unit Coming of Age: a Journey through Neurovascular Coupling in Health and Disease. Neuron 2017;96:17–42.
3. Chabriat H, Joutel A, Dichgans M, et al. Cadasil. Lancet Neurol 2009;8:643–653.
4. Tournier-Lasserve E, Joutel A, Melki J, et al. Cerebral autosomal dominant arteriopathy with subcortical infarcts and leukoencephalopathy maps to chromosome 19q12. Nat Genet 1993;3:256–259.
5. Monet-Lepretre M, Haddad I, Baron-Menguy C, et al. Abnormal recruitment of extracellular matrix proteins by excess Notch3 ECD: a new pathomechanism in CADASIL. Brain 2013;136(Pt 6):1830–1845.
6. Capone C, Dabertrand F, Baron-Menguy C, et al. Mechanistic insights into a TIMP3-sensitive pathway constitutively engaged in the regulation of cerebral hemodynamics. ELife 2016;5: pii: e17536.
7. Joutel A, Monet-Lepretre M, Gosele C, et al. Cerebrovascular dysfunction and microcirculation rarefaction precede white matter lesions in a mouse genetic model of cerebral ischemic small vessel disease. J Clin Investig 2010;120:433–445.
8. Dabertrand F, Kroigaard C, Bonev AD, et al. Potassium channelopathy-like defect underlies early-stage cerebrovascular dysfunction in a genetic model of small vessel disease. Proc Natl Acad Sci USA 2015;112:E796–E805.
9. Arthurs OJ, Williams EJ, Carpenter TA, et al. Linear coupling between functional magnetic resonance imaging and evoked potential amplitude in human somatosensory cortex. Neuroscience 2000;101:803–806.
10. Dumas A, Dierksen GA, Gurol ME, et al. Functional magnetic resonance imaging detection of vascular reactivity in cerebral amyloid angiopathy. Ann Neurol 2012;72:76–81.
11. Tak S, Yoon SJ, Jang J, et al. Quantitative analysis of hemodynamic and metabolic changes in subcortical vascular dementia using simultaneous near-infrared spectroscopy and fMRI measurements. NeuroImage 2011;55:176–184.
12. Buxton RB. Dynamic models of BOLD contrast. NeuroImage 2012;62:953–961.
13. Zhao F, Wang P, Kim SG. Cortical depth-dependent gradient-echo and spin-echo BOLD fMRI at 9.4T. Magn Reson Med 2004;51:518–524.
14. Lee SP, Duong TQ, Yang G, et al. Relative changes of cerebral arterial and venous blood volumes during increased cerebral blood flow: implications for BOLD fMRI. Magn Reson Med 2001;45:791–800.
15. Wu WC, Fernandez-Seara M, Detre JA, et al. A theoretical and experimental investigation of the tagging efficiency of pseudocontinuous arterial spin labeling. Magn Reson Med 2007;58:1020–1027.
16. Petersen ET, Zimine I, Ho YC, Golay X. Non-invasive measurement of perfusion: a critical review of arterial spin labelling techniques. Br J Radiol 2006;79:688–701.
17. Wong EC, Buxton RB, Frank LR. Implementation of quantitative perfusion imaging techniques for functional brain mapping using pulsed arterial spin labeling. NMR Biomed 1997;10:237–249.
18. Mullinger KJ, Mayhew SD, Bagshaw AP, et al. Poststimulus undershoots in cerebral blood flow and BOLD fMRI responses are modulated by poststimulus neuronal activity. Proc Natl Acad Sci USA 2013;110:13636–13641.
19. Bell AJ, Sejnowski TJ. An information-maximization approach to blind separation and blind deconvolution. Neural Comput 1995;7:1129–1159.
20. Perlbarg V, Marrelec G, Doyon J, et al. NEDICA: Detection of group functional networks in FMRI using spatial independent component analysis," 2008.
21. Cook R, Weisberg S. Residuals and influence in regression. 1st ed. New York: Chapman and Hall, 1982.
22. Bates D, Mächler M, Bolker B, Walker S. Fitting Linear Mixed-Effects Models Using lme4. J Stat Softw 2015;67: i01.
23. Allen PJ, Josephs O, Turner R. A method for removing imaging artifact from continuous EEG recorded during functional MRI. NeuroImage 2000;12:230–239.
24. Oostenveld R, Fries P, Maris E, Schoffelen JM. FieldTrip: open source software for advanced analysis of MEG, EEG, and invasive electrophysiological data. Comput Intell Neurosci 2011;2011:156869.
25. Fox PT, Raichle ME. Stimulus rate dependence of regional cerebral blood flow in human striate cortex, demonstrated by positron emission tomography. J Neurophysiol 1984;51:1109–1120.
26. Nakamura M, Kakigi R, Okusa T, et al. Effects of check size on pattern reversal visual evoked magnetic field and potential. Brain Res 2000;872:77–86.
27. Seki Y, Miyashita T, Kandori A, et al. Simultaneous measurement of neuronal activity and cortical hemodynamics by unshielded magnetoencephalography and near-infrared spectroscopy. J Biomed Optics 2012;17:107001.


 

28. Shigeto H, Tobimatsu S, Yamamoto T, et al. Visual evoked cortical magnetic responses to checkerboard pattern reversal stimulation: a study on the neural generators of N75, P100 and N145. J Neurol Sci 1998;156:186–194.
29. Tuominen S, Miao Q, Kurki T, et al. Positron emission tomography examination of cerebral blood flow and glucose metabolism in young CADASIL patients. Stroke 2004;35:1063–1067.
30. Parisi V, Pierelli F, Malandrini A, et al. Visual electrophysiological responses in subjects with cerebral autosomal arteriopathy with subcortical infarcts and leukoencephalopathy (CADASIL). Clin Neurophysiol 2000;111:1582–1588.
31. Capone C, Cognat E, Ghezali L, et al. Reducing Timp3 or vitronectin ameliorates disease manifestations in CADASIL mice. Ann Neurol 2016;79:387–403.
32. Longden TA, Dabertrand F, Koide M, et al. Capillary K + -sensing initiates retrograde hyperpolarization to increase local cerebral blood flow. Nat Neurosci 2017;20:717–726.
33. Lind BL, Brazhe AR, Jessen SB, et al. Rapid stimulus-evoked astrocyte Ca2 + elevations and hemodynamic responses in mouse somatosensory cortex in vivo. Proc Natl Acad Sci USA 2013;110:E4678–E4687.
34. Schulz K, Sydekum E, Krueppel R, et al. Simultaneous BOLD fMRI and fiber-optic calcium recording in rat neocortex. Nat Methods 2012;9:597–602.
35. Mishra A, Reynolds JP, Chen Y, et al. Astrocytes mediate neurovascular signaling to capillary pericytes but not to arterioles. Nat Neurosci 2016;19:1619–1627.
36. Rosenegger DG, Gordon GR. A slow or modulatory role of astrocytes in neurovascular coupling. Microcirculation 2015;22:197–203.
37. Joutel A, Andreux F, Gaulis S, et al. The ectodomain of the Notch3 receptor accumulates within the cerebrovasculature of CADASIL patients. J Clin Investig 2000;105:597–605.
38. Cheema I, Switzer AR, McCreary CR, et al. Functional magnetic resonance imaging responses in CADASIL. J Neurol Sci 2017;375:248–254.
39. Peca S, McCreary CR, Donaldson E, et al. Neurovascular decoupling is associated with severity of cerebral amyloid angiopathy. Neurology 2013;81:1659–1665.

 